Anomalous temperature dependence of electrical transport in quantum Hall multilayers

H. A. Walling,[1] D. P. Dougherty,[1] D. P. Druist,[1] E. G. Gwinn,[1] K. D. Maranowski,[2] and A. C. Gossard[2]
[1]*Physics Department, University of California, Santa Barbara, California 93106, USA*
[2]*Materials Department, University of California, Santa Barbara, California 93106, USA*
(Received 16 December 2003; revised manuscript received 19 March 2004; published 20 July 2004)

We study the temperature dependence of vertical transport through the chiral sheath of surface states that exists near the sidewalls of GaAs/$Al_{0.01}Ga_{0.09}As$ multilayer structures in the regime of the integer quantum Hall effect. Because variable-range hopping through the bulk provides a parallel conduction channel, we design our experiment to extend the temperature range of sheath-dominated transport. To do so, we increase device perimeter by using fractal-perimeter mesas. We report on the nearly linear increase of the sheath conductivity with temperature, a result not predicted by existing theories for the edge state sheath.

DOI: 10.1103/PhysRevB.70.045312 PACS number(s): 73.21.Ac, 73.43.−f

A two-dimensional (2D), chiral sheath of surface states exists near the sidewalls of multilayer semiconductor mesas in the regime of the integer quantum Hall effect.[1] Fermi-level states within the bulk of the multilayer are localized at low temperatures, so transport perpendicular to the plane of the layers occurs primarily via the edge states of the quantum wells. As electrons tunnel between layers, the edge states couple weakly to form the surface sheath [Fig. 1(a)]. Transport on the sheath is ballistic in the plane of the quantum wells, diffusive in the perpendicular direction,[2] and chiral because electrons circle the mesa in one direction only. An electron circling the mesa cannot backscatter, so if the mesa perimeter is large enough to preclude coherent transport around the perimeter, the system will not localize.[3] This suppression of localization makes the chiral sheath an interesting experimental test bed for understanding the different factors that influence electrical transport in low-dimensional systems.

Here, we use an MBE-grown GaAs/AlGaAs multilayer structure that we patterned into optimized geometries to study the temperature (T) dependence of the vertical conductivity, σ_{sheath}, of this unusual 2D system.[4] Because the mesas we study have large perimeters, the observed temperature dependence should not exhibit localization physics, but instead will reflect disorder, inelastic, and interaction effects in this chiral tunneling system.[5,6] Although edge states in the integer quantum Hall effect are well-studied and are thought to have simple physics,[7–10] the behavior we observe in $\sigma_{\text{sheath}}(T)$ is unexpected and points to inelastic or interaction effects that have not been considered previously. Our results are of general interest as a complementary probe of transport physics to the more heavily studied isotropic 2D systems.

Early work on GaAs/A1GaAs multilayers established that in-plane transport measurements in the quantum Hall (QH) regime yield results qualitatively similar to the QH effect in a single 2D system: plateaus in the Hall resistance (R_H) accompany vanishing longitudinal resistance.[11] Quantum Hall states in vertical transport measurements are characterized by minima in the vertical conductance, G_{zz}, that correspond to the in-plane plateaus in R_H.[1] Size scaling experiments on vertical transport mesas showed that at low T in QH states, G_{zz} is proportional to the mesa perimeter, P. At higher temperatures, transport through the bulk dominates and G_{zz} is proportional to the sample area, A.[1]

At any nonzero temperature, parallel transport through the bulk contributes to the total vertical conductance. We therefore model the measured conductance, G_{zz}, as the sum of a sheath conductance, $G_{\text{sheath}}=(P/H)\sigma_{\text{sheath}}$, and a bulk conductance, $G_{\text{bulk}}=(A/H)\sigma_{\text{bulk}}$, where H is the height of the multilayer. Because the sheath conductivity, σ_{sheath}, has a weak temperature dependence compared to the bulk conductivity, σ_{bulk}, we must take care to distinguish the temperature dependence of σ_{sheath} from that of σ_{bulk}. We design our experiment to maximize the temperature range of sheath-dominated transport, while remaining in the incoherent limit so that localization effects are negligible.

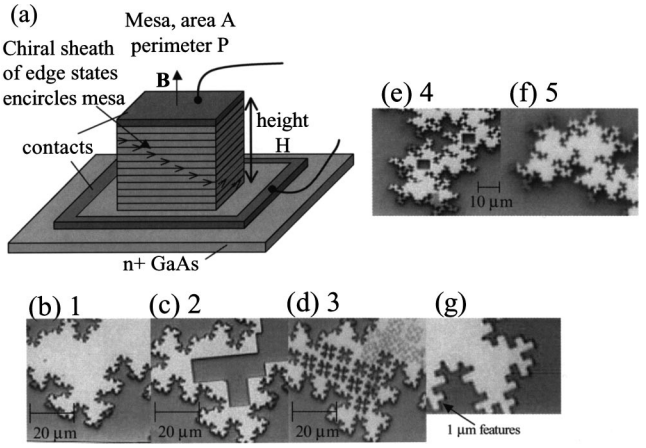

FIG. 1. (a) Schematic of samples used to study sheath transport. (b)–(f) Top-view micrographs of samples show roughly 1/4 of the sample area. Light areas are the gold-covered mesas. Dark areas are the etched wafer. In sample 3, light-colored features are fractal-shaped holes where the contact metal did not lift off before the mesa was etched. These areas are therefore not etched and do not affect the total sample perimeter or area. Dark, square-shaped features in samples 2 and 4 are holes etched into the fractal-shaped mesas. These regions decrease overall sample area and increase perimeter. In all samples, there are areas (darker) where the mesa etch removed some of the contact gold near the sample edges. (g) All samples have 1-μm minimum features.

 ©2004 The American Physical Society

TABLE I. Total perimeters, areas, and α for the samples studies.

Sample number	Perimeter (μm)	Area (μm^2)	α
1	16 384±650	65 536	1.21±0.14
2	18 000±720	40 000	0.89±0.42
3	22 272±890	59 648	1.26±0.32
4	4 146±170	4 046	0.99±0.10
5	4 096±170	4 096	1.01±0.38
5 (second time)	4 096±170	4 096	1.31±0.21

Earlier work used a different approach to estimate $\sigma_{\text{sheath}}(T)$ in a similar multilayer structure, and did not analyze the low-T limit that is the focus of this work.[4] This group fabricated two mesas with the same area, but different perimeters. They assumed the high-T bulk contributions would be identical, and thus interpreted the difference of the two data sets as $\sigma_{\text{sheath}}(T)$. This work assumed negligible variation in materials properties across the semiconductor wafers. We do not make this assumption, and instead exploit the geometry of our mesas to maximize sensitivity to σ_{sheath}, for temperatures between 50 and 300 mK. This method allows us to characterize G_{zz} in the sheath-dominated transport regime without complicating the analysis with a subtraction procedure. A preliminary report on part of the data has appeared elsewhere.[12]

Our strategy for optimizing sensitivity to sheath properties is to increase P by using mesas with fractal perimeters. Figures 1(b)–1(f) show a top-view photograph of one quadrant of each of the five mesas studied. Fractals 1, 2, and 3 have identical outer perimeters of fractal dimension $d=1.5$. Samples 2 and 3 have holes removed from their interiors, resulting in larger total perimeters and smaller areas than sample 1. Samples 4 and 5 have identical outer perimeters with $d=1.67$, but different total P and A. Table I gives total P and A for the five samples. The minimum feature size for all of the fractals is 1 μm [Fig. 1(g), a blow-up of one region, displays the quality of the lithography].

A different way to maximize P relative to A is to make samples with small P. The problem with this approach is that localization effects are expected in samples small enough that electrons can circumnavigate the perimeter phase coherently.[13,14] Our fractals have large enough P (to $\sim$2 mm) that such circumnavigation is highly unlikely. Since we observe similar behavior in samples with P spanning a factor of 4, localization effects from phase-coherent wrapping paths appear negligible at the size scales studied.

We fabricated all samples from a multilayer structure with 160 periods of 150 Å GaAs quantum wells alternating with 150 Å $Al_{0.1}Ga_{0.9}As$ barriers. Thus the multilayer height, H, of all mesas is 4.79 μm. The barriers are Si-doped at their centers to give the quantum wells a sheet density of 3.4×10^{11} cm^{-2}, as extracted from in-plane transport experiments on a companion structure. In the vertical transport samples, there is a layer of degenerately doped $n+$GaAs above and below the top and bottom $Al_{0.1}Ga_{0.9}As$ layers, to which we made Ohmic electrical contacts using alloyed NiAuGe. We defined the fractal mesas with e-beam lithography and deposited the contact metal to act as both an etch mask and Ohmic top contacts. To give the mesas vertical walls we dry etched the sample in a reactive ion etcher, using $SiCl_4$. We used photolithography to define the bottom contacts for lift-off, and deposited NiAuGe. We alloyed the top and bottom contacts for 1 min at 430°C in a rapid thermal annealer. Finally, we deposited a thick layer of Ti/Au to allow wire bonding. We relied on the Schottky barrier in GaAs not to short the layers together.

We conducted our experiment twice, thermally cycling the samples between runs. We measured samples 1, 3, and 5 over a temperature range from 50 mK to 2 K during the first run, and 2, 4, and 5 from 50 mK to 1.3 K during the second. We repeated measurements of sample 5 to observe the effects of thermal cycling on our results. We used small excitation currents to measure the vertical conductance, G_{zz}, of the mesas at dilution refrigerator temperatures, taking care to ensure linear IV characteristics at 50 mK. Measurement signals corresponded to $\sim10^{-15}$ W at 50 mK. We applied a magnetic field perpendicular to the layers and swept it slowly from 0–17.9 T to locate the quantum Hall states. At low temperatures, we found $G_{zz}\propto P$ within QH states; at high temperatures, $G_{zz}\propto A$ for all fields. The temperature scale for the crossover from bulk-dominated ($G_{zz}\propto A$) to sheath-dominated ($G_{zz}\propto P$) transport depends on the sample geometry, but is on the order of 500 mK at the center of the $\upsilon=2$ per layer quantum Hall state, which was well-defined for all of the mesas. We set the magnet to the center of this state, $B=6.75$ T, and proceeded to sweep the temperature from 50 mK to 2 K. See Fig. 1 of Ref. 12 for a magnetic field sweep between 0 and 17 T that shows the center of the $\upsilon=2$ QH state. Here, we use υ to denote the number of filled Landau bands below the Fermi energy rather than the filling factor.

To display the quality of size scaling at low temperatures, Fig. 2(a) shows a log-log plot of G_{zz} versus sample perimeter, P, for samples 1–5 at $T=100$ mK. The line with slope 1 on this log-log plot shows good overall agreement with $G_{zz}\propto P$. For comparison, the inset in Fig. 2(a) shows G_{zz} versus sample area, A, at 100 mK. Comparison to the line with slope 1 in the inset shows that G_{zz} does not scale with A in the limit of low temperatures. To display the quality of size scaling at high temperatures, Fig. 2(b) shows a log-log plot of G_{zz} versus sample area, A, for the five samples at $T=1.34$ K. The line with slope 1 on this log-log plot shows good overall agreement with $G_{zz}\propto A$ at 1.34 K. The inset in Fig. 2(b) shows a log-log plot of G_{zz} versus P at 1.34 K. The line with slope 1 in the inset shows that at this high temperature, G_{zz} is not proportional to P.

Figures 3(a) and 3(b) show G_{zz} as a function of temperature for samples 1, 3 and 5 (2 and 4). For all five samples G_{zz} is weakly temperature dependent below $\sim$500 mK and rises rapidly at higher temperatures, where bulk transport dominates. Figure 4 plots the low-T sheath conductivity, σ_{sheath}, estimated from the low-T G_{zz} using $\sigma_{\text{sheath}}=HG_{zz}/P$, where H is the sample height and P is the perimeter.

As shown in Fig. 4, for all samples σ_{sheath} rises roughly linearly at low T, with similar slopes. The standard deviation of the intercept is $\sim$4%. We believe that this spread is due to

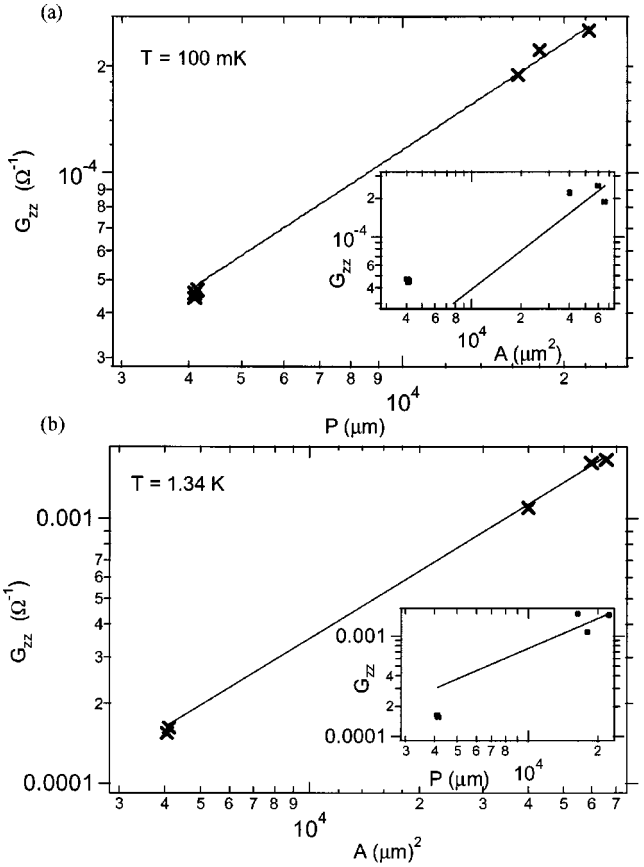

FIG. 2. (a) Log-log plot of G_{zz} versus sample perimeter (P) for samples 1–5 at $T=100$ mK. The line with slope=1 indicates that $G_{zz} \propto P$ at low temperatures. The inset shows a log-log plot of G_{zz}versus sample area at $T=100$ mK. The solid line with slope=1 shows that at low temperatures, G_{zz} is not proportional to A. (b) Log-log plot of G_{zz} versus sample area (A) for samples 1–5 at $T=1.34$ K. The solid line with slope=1 shows that at high temperatures, $G_{zz} \propto A$. The inset shows a log-log plot of G_{zz} versus sample perimeter at $T=1.34$ K. The solid line with slope=1 shows that at high temperatures, G_{zz} is not proportional to P.

a combination of factors, including an approximately 4% uncertainty in the sample perimeters, based upon high-magnification photographs of our samples. These images show slight rounding at the sample corners that accounts for <1% uncertainty. In addition, the long mesa etch removed the contact metal from some regions of the sample edges, as shown by the small, darker gray areas at the mesa edges in Fig. 1(b). This likely caused some degree of sample erosion in the affected regions. We estimate that this effect adds a maximum of 4% uncertainty in P. Uncertainty in the sample area due to such perimeter imperfections or to errors in field stitching during electron-beam lithography is negligible. Gradients over the wafer during MBE growth that slightly change barrier and well thicknesses provide an additional source of variability between samples. Because the alignment of edge states between layers affects the strength of tunneling, mesa sidewalls that are not perfectly flat will produce stronger tunneling at points where the edge states overlap. Thus, variations in flatness of the sidewall profile between mesas may also contribute to the spread in σ_{sheath}.

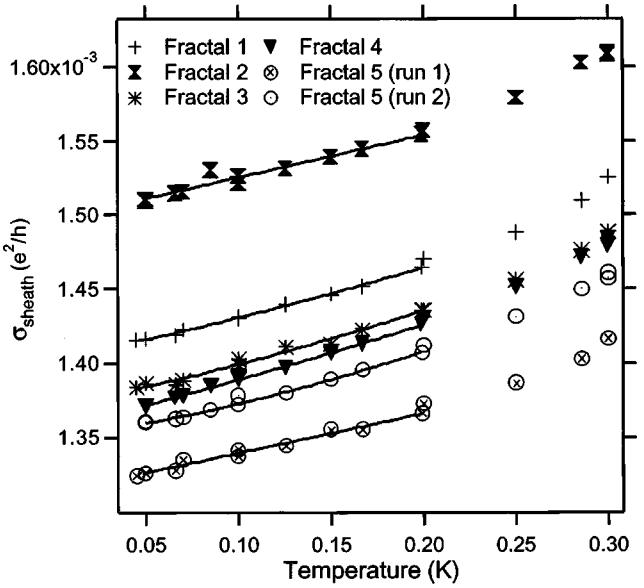

FIG. 4. Vertical sheath conductivity, $\sigma_{\text{sheath}}=HG_{zz}/P$, for all samples, in units of e^2/h. The sheath conductivity initially rises approximately linearly with temperature. The solid lines are fits to $G_{zz}=G_0+K_1T^{\alpha}$ between 50–200 mK. The α values are given in Table I and the text.

To be sure that the observed weak temperature dependence in G_{zz} below ~500 mK was not the result of poor thermal contact between the sample and the mixing chamber of the dilution refrigerator, we used the mesa with the largest area A to P ratio ($A/P=4$ μm), sample 1, as a thermometer. Because the $\nu=4$ QH state becomes developed at lower temperatures than for $\nu=2$, we expected transport to be dominated by the bulk in the $\nu=4$ quantum Hall state (3.55 T) at

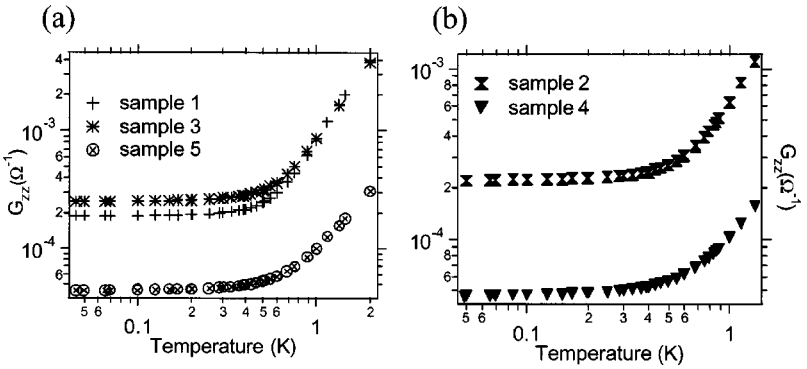

FIG. 3. (a) G_{zz} versus temperature at 6.75 T for fractals 1, 3, and 5. (b) G_{zz} versus temperature at 6.75 T for fractals 2 and 4. G_{zz} is weakly T dependent below ~500 mK and then rises rapidly with temperature.

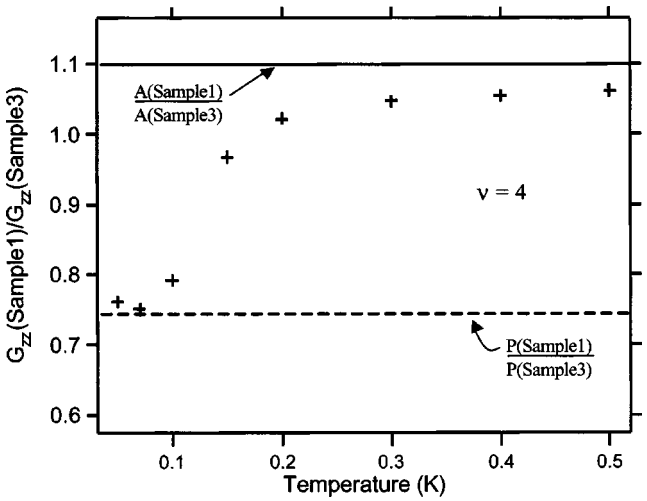

FIG. 5. Symbols show the ratio of G_{zz} for sample 1 to G_{zz} for sample 3. At high temperatures this ratio approaches the solid horizontal line, which shows the ratio of the area of sample 1 to the area of sample 3. At temperatures below 100 mK, the data approach the dashed horizontal line, which shows the ratio of the perimeter of sample 1 to the perimeter of sample 3. This crossover in size scaling indicates a crossover to sheath-dominated transport at low temperatures.

all but the lowest temperatures, with corresponding strong temperature dependence in G_{zz} due to the dominance of hopping transport through the bulk. This was the case from 2 K to ~100 mK: G_{zz} followed a variable-range hopping (VRH) temperature dependence. At lower temperatures G_{zz} fell more slowly, and showed a crossover in size scaling from $G_{zz} \propto A$ to $G_{zz} \propto P$, indicating that the bulk contribution had become negligible. To illustrate this bulk-to-sheath crossover, Fig. 5 shows the ratio of G_{zz} for sample 1 to G_{zz} for sample 3 in the center of the $\nu=4$ QH state (3.55 T). We expected this ratio to equal the ratio of the two samples' perimeters only at very low temperatures. The solid horizontal line shows the ratio of the area of sample 1 to the area of sample 3, and the dashed horizontal line shows the ratio of the perimeter of sample 1 to the perimeter of sample 3. The data approach the solid line at high temperatures and the dashed line at low temperatures, indicating a crossover to sheath-dominated transport at temperatures less than 100 mK. We therefore concluded that the electrons reached temperatures below 100 mK. Thus, we are confident that the data's behavior at low temperatures is not a result of poor equilibration with the mixing chamber.

As an initial investigation of the temperature dependence of sheath conduction, we fit the data to $G_{zz}=G_{\text{sheath}}+G_{\text{bulk}}$ with $G_{\text{sheath}}=G_0+K_1T^{\alpha}$, where G_0 is the zero-temperature sheath conductance. To account for parallel transport through the bulk, we used a VRH form that fits the bulk well at high T, $G_{\text{bulk}}=K_2T^{\beta}\exp[-(T_0/T)^{\gamma}]$, with $\gamma=1/2$ for the bulk hopping exponent.

Figure 6 shows that the observed weakly temperature-dependent behavior that we find at low temperatures is characteristic of the edge state sheath and not a remnant contribution from bulk hopping. The low-T data points are for sample 1 and the dashed line is G_0+G_{bulk}, with G_{bulk} the VRH form fitted to the high-T data. As shown, the variation

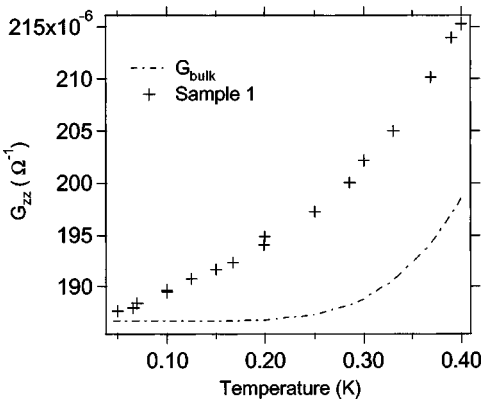

FIG. 6. Variable-range hopping form as a function of temperature compared to experimental data (symbols). The dashed line has $\gamma=1/2$. The VRH form has a much weaker temperature dependence at low temperatures than the data.

in G_{bulk} is negligible relative to the observed temperature dependence for temperatures below ~300 mK. We have tested that the value of the bulk hopping exponent γ does not strongly affect fits to the bulk conductance: values of $\gamma=1,1/3$, and $1/4$ all give a fitted G_{bulk} that makes negligible contribution to G_{zz} below ~300 mK.

After we characterized the bulk and determined that the data's weak temperature dependence at low temperatures was not simply a remnant bulk contribution, we assumed $G_{zz} \cong G_{\text{sheath}}$ and fit the low-T data for all five fractals to $G_{zz}=G_0+K_1T^{\alpha}$. Fits from 50–200 mK, a range over which the bulk contribution is negligible, give $\alpha=1.11\pm0.17$ as the average and standard deviation over all samples. Table I lists the values of α for each sample and the corresponding fit uncertainties.

The fits to the low-T data show that σ_{sheath} rises roughly linearly with temperature. Because the fitted exponent α is slightly greater than 1, and because the data have an upward curvature at temperatures at which we expect negligible bulk contribution, the sheath conductance is perhaps a power series with the linear term dominating at the lowest temperatures accessed by our experiment.

To observe the effects of thermal cycling on our measurements, we compared $G_{zz}(T)$ for fractal 5 for both data sets. We found good agreement at low temperatures. Fitting the low-T data (to 300 mK) to a straight line yields slopes and 0-K intercepts that agree within 2%, indicating a high degree of reproducibility of sheath conductivity with thermal cycling. High-T transport exhibits larger changes with thermal cycling, with bulk hopping slightly stronger for the second data set than the first. The boundaries of the QH states change slightly between thermal cycles, so this sensitivity of bulk transport to thermal cycling may reflect corresponding changes in the bulk localization length,[15] to which hopping transport is quite sensitive.

Although we concentrated our studies on the center of the $\nu=2$ QH state (6.75 T), we also studied $\sigma_{\text{sheath}}(T)$ at off-center magnetic field values, at $B=6.25$ T and $B=7.0$ T. At 7.0 T, $G_{zz}(T)$ closely resembles $G_{zz}(T)$ at 6.75 T, but has a slightly smaller low-T slope. The 6.25-T data show that at this field the bulk contribution grows much faster than at

6.75 and 7 T, presumably reflecting an enhancement of the bulk localization length at fields closer to the transition between QH states. We note that other groups[16,17] have studied the breakdown of the QHE in the regime of nonlinear, in-plane transport in single 2-dimensional electron gas. Because we take measurements well within the regime of linear response, and because our vertical transport experiments do not give rise to a transverse Hall voltage, we believe that the more rapid rise in conductance that we observe away from integer v is not related to the breakdown of the QHE that these groups studied.

The nearly linear increase in σ_{sheath} with temperature is surprising. Barely metallic, three-dimensional systems have shown similar temperature dependence in the vicinity of a metal-insulator transition;[18] however, the nature of electron trajectories in such systems is quite different from chiral flow on the sheath, and we see no reason to expect similar dependence on temperature. Theory for the chiral sheath predicts that interactions in weakly coupled quantum wells give $\sigma_{\text{sheath}}=\sigma_0+KT^2$, with K negative.[14] Apparently factors not included in present theory are important in transport on the surface sheath.

To attempt to understand our results, we used a simple, noninteracting model to investigate the temperature dependence of the tunneling conductance, G, through a barrier with energy-dependent transmission $T(E)$. In such a system $G \propto \int T(E)g(E)(-\partial f/\partial E)dE$, where f is the Fermi-Dirac function. We assumed $g(E)$, the density of states, to be energy independent, and approximated $T(E)$ using the WKB method for our quantum-well barriers to calculate the integral. The result was a calculated increase in G_{zz} of 7×10^{-4} % between 50 and 300 mK. Our experimentally observed G_{zz} increases by $\sim$10% over the same temperature range. We conclude that thermal broadening effects on tunneling are too weak to explain our much stronger observed temperature dependence.

We also considered inelastic effects that disorder could produce in interlayer tunneling in our system. Impurity potentials will cause the edge states to meander relative to one another, producing maxima in the tunneling rate in regions where edge states overlie. This meandering of edges produces a shift in the dispersion relations in adjacent layers. If we consider two straight sections where the edges of adjacent layers are separated by s, their dispersion relations acquire a relative momentum shift $q(s)=s/\ell m^2$, where ℓ_m is the magnetic length. As a result, momentum and energy cannot be conserved simultaneously. To tunnel between layers and conserve momentum, electrons must gain energy from some source: scattering from phonons or from other electrons. Qualitatively, we expect this inelastic scattering would cause σ_{sheath} to rise with increasing temperature, though we do not know its functional form. We note that electron-phonon interactions are predicted to destroy the Fermi-liquid state at integer filling in single 2DEG systems,[19] and thus may have important effects here.

Alternatively, electron-electron interaction effects, such as scattering from collective excitations or energy-dependent density of states (DOS) at E_F, could perhaps result in a linear increase in σ_{sheath} with temperature over the range observed in the data. Energy-dependent DOS commonly arises in diffusive systems, though no estimates of similar effects on the conductivity of chiral systems are available.

In summary, low-temperature transport perpendicular to the layers of a multilayer quantum Hall system showed an unexpected temperature dependence. In the absence of inelastic and interaction effects, the vertical conductivity of the sheath, σ_{sheath}, would be independent of temperature. Theory that assumes a constant density of states predicts interaction effects to produce a quadratic fall in σ_{sheath} with temperature. Instead, we observe a linear increase in σ_{sheath} at low temperatures, with a slope that is too large to explain by thermal broadening.

We thank R. Sedgewick for writing code to generate the fractal images that we used to fabricate our mesas. We thank John Chalker, Matthew Fisher, and Leon Balents for helpful conversations, and Ernie Caine for help with the electron-beam lithography. This work was supported by NSF-DMR 9700767 and NSF-DMR 0071956.

[1] D. P. Druist, P. J. Turley, E. G. Gwinn, K. D. Maranowski, and A. C. Gossard, Phys. Rev. Lett. **80**, 365 (1998).
[2] L. Balents and M. P. A. Fisher, Phys. Rev. Lett. **76**, 2782 (1996).
[3] J. T. Chalker and A. Dohmen, Phys. Rev. Lett. **75**, 4496 (1995).
[4] M. Kuraguchi and T. Osada, Physica E (Amsterdam) **6**, 594 (2000).
[5] J. T. Chalker and S. L. Sondhi, Phys. Rev. B **59**, 4999 (1999).
[6] J. J. Betouras and J. T. Chalker, Phys. Rev. B **62**, 10931 (2000).
[7] B. I. Halperin, Phys. Rev. B **25**, 2185 (1982).
[8] A. H. Macdonald and P. Streda, Phys. Rev. B **29**, 1616 (1984).
[9] B. E. Kane, D. C. Tsui, and G. Weimann, Phys. Rev. Lett. **59**, 1353 (1987).
[10] R. J. Haug, Semicond. Sci. Technol. **8**, 131 (1993).
[11] H. L. Stormer, J. P. Eisenstein, A. C. Gossard, W. Wiegmann, and K. Baldwin, Phys. Rev. Lett. **56**, 85 (1986).
[12] H. A. Walling, D. P. Dougherty, D. P. Druist, E. G. Gwinn, K. D. Maranowski, and A. C. Gossard, Physica E (Amsterdam) **12**, 132 (2002).
[13] I. A. Gruzberg, N. Read, and S. Sachdev, Phys. Rev. B **56**, 13218 (1997).
[14] S. Cho, L. Balents, and M. P. A. Fisher, Phys. Rev. B **56**, 15814 (1997).
[15] M. Furlan, Phys. Rev. B **57**, 14818 (1998), and references therein.
[16] G. Nachtwei, Physica E (Amsterdam) **4**, 79 (1999).
[17] L. B. Rigal, D. K. Maude, M. Potemski, J. C. Portal, L. Eaves. Z. R. Wasilewski, G. Hill, and M. A. Pate, Phys. Rev. Lett. **82**, 1249 (1999).
[18] M. A. Dubson and D. F. Holcomb, Phys. Rev. B **32**, 1955 (1985).
[19] O. Heinonen and S. Eggert, Phys. Rev. Lett. **77**, 358 (1996).